

DYNAMIC DRIVERS OF TIFE DIURNAL CYCLE IN ANTARCTICA

Zhibin Yu^{1,2*}, Xinzhao Chu², Xian Lu², and Cao Chen²

¹Harbin Institute of Technology (Shenzhen), Guangdong 518055, China. *Email: yuzb@hit.edu.cn

²University of Colorado Boulder, Colorado 80309, USA

ABSTRACT

The discovery of the thermosphere-ionosphere Fe (TIFE) layers has opened a door to exploring the least understood thermosphere and ionosphere region between 100 and 200 km with ground-based lidar instruments. The characteristics of the polar TIFE layers, and the impacts of the atmosphere neutral dynamics, electrodynamics, and metallic chemistry on the formation of TIFE layers deserve further investigation, especially the diurnal cycles of TIFE layers observed by lidar. This paper aims at investigating the major driving forces with 1-D Thermosphere-Ionosphere Fe/Fe⁺ (TIFE) model. A main question to answer is whether neutral dynamics like tidal winds or electrodynamics like the convection electric fields and currents in the magnetosphere and ionosphere are responsible for the diurnal cycle of TIFE layers.

1. INTRODUCTION

As the lower boundary of space weather regime, the region between 100 and 200 km is one of the key regions for the coupling among the neutral-ion chemistry, neutral dynamics, and ionospheric electrodynamics. Atmospheric waves of upward propagation transport energy and momentum and cause strong disturbances in the 100–200 km region [1, 2]. In polar region, energetic particle precipitations have substantial impacts on the properties of the neutrals and plasma in the upper atmosphere and ionosphere via direct ionization. However, due to lack of observations, 100–200 km region is still one of the least understood regions in the upper atmosphere.

The first TIFE layers up to 155 km discovered by Prof. Xinzhao Chu's group at Antarctica exhibit clear gravity wave structures with ~1.5 h period [3]. These thermospheric metal layers provide excellent traces for studying the coupling among neutral dynamics, chemistry, and electrodynamics in the E and lower F regions of ionosphere. Numerous studies based on lidar observations and numerical simulations have contributed to our understandings of the chemical and dynamical

processes of the main metal layers distributing between around 70 km and 110 km [4]. The fundamental differences in the characteristics of the main metal layers and thermospheric metal layers give rise to non-available theory that could be directly applied to explain the formation of the thermospheric metal layers.

Chu et al. [3] originally hypothesize that the thermospheric Fe layers are formed through the direct recombination of the electrons with Fe⁺ ions. These ions are uplifted by the polar electric field from the main deposition region to E-F region and vertically converged by neutral wind and electric field. This qualitative explanation is supported by the numerical simulations using a thermosphere-ionosphere Fe/Fe⁺ (TIFE) model [Chu and Yu, 2017], which provide a detailed quantitative explanation of the gravity-wave-shaped Fe layers. The vertical wind shear generated by gravity waves appears to be the dominant factor to converge Fe⁺ ions redistributed from the main deposition region to the upper regions by the convective electric field. The energetic particles originated from the magnetosphere substantially increase the electron density, enhancing the speed of direct recombination between Fe⁺ and electrons.

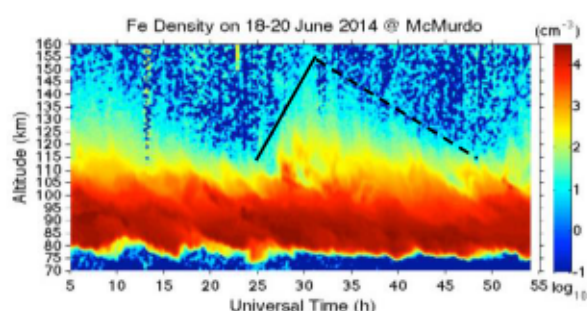


Fig. 1. Periodic diurnal cycles of the thermospheric Fe layers during a continuous 50 h of lidar observations at McMurdo, reproduced from Chu et al. [2016].

Besides the gravity-wave-shaped thermospheric metal layers, tidal-shaped thermospheric metal layers have been observed globally by the recent lidar studies [6, 7, 8, 9]. Unlike the diffused topside metal layer observed by Höffner and Friedman [10, 11], the density perturbations of the

high-altitude TIFe layers show clear downward phase propagation with tidal or gravity-wave period. The thermospheric K layer reported from Arecibo descended with a similar speed as the downward phase speed of the modeled semidiurnal tide over Arecibo [6], so does the thermospheric Na layers reported from Lijiang, China [7] and Cerro Pachón, Chile [8]. The phase speed consistency strongly implies the essential roles played by the tidal-wave-generated winds in the formation of the thermospheric metal layers in the mid and low latitudes. However, the diurnal variations of the thermospheric Fe layers at Antarctica showed in Lübken et al. [2011] and Chu et al. [2016] exhibits more complex features rather than just downward phase speed of tides.

In this paper, we adopt the 1-D TIFe model to investigate the roles of the tidal winds and convective electric field in the formation of the diurnal features of the TIFe layers in Antarctica.

2. OBSERVATIONS

The Fe Boltzmann temperature lidar installed at Arrival Heights Observatory (77.8°S, 166.7°E) by the University of Colorado Boulder has been described in Chu et al. [2011, 2016]. The unique location of the Arrival Heights enables that the lidar observations produce outstanding datasets, leading to several scientific breakthroughs [13]. The nearly-zero artificial light pollution reduce the background noise to the lowest level so that the lidar system is sensitive to very low Fe density under relatively short integration time. The extended darkness during the polar nights enabled the continuous observations of TIFe layers over two days. Such data runs have benefitted greatly from the hard work of winter-over lidar students.

A diurnal TIFe layer case is the 50-h continuous Fe observations taken by Dr. Cao Chen in June 2014 at McMurdo (see Figure 1). Variations of TIFe layers clearly present diurnal features associated with the highest layer around 8 and 32 UT at 150–160 km. Before 8 UT, the peak altitudes of the three thermospheric Fe layers gradually increase from 115 to 150 km and then descend with relatively slower speed. Eventually the envelope of the thermospheric Fe layers forms a shape similar to a skewed Gaussian profile. The upward extension of the thermospheric Fe layers is ascending at the rate of ~ 1.4 m/s (the solid

black line in Figure 1), and descending rate is ~ 0.7 m/s (the dashed black line). Within a single envelope of the thermospheric Fe layer, the Fe densities are perturbed by several cycles of short-period gravity waves, which clearly show downward phase progression.

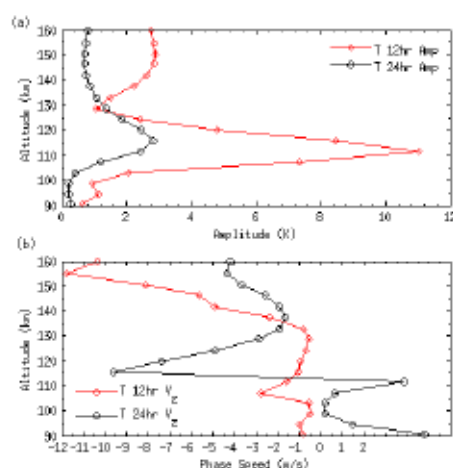


Fig. 2. (a) Amplitudes of diurnal temperature tides (black) and semidiurnal temperature tides (red), (b) the corresponding vertical phase speeds computed by GSWM09 in June at McMurdo.

The descending rate (the dashed black line in Figure 1) is much slower than the gravity-wave phase speed in the thermospheric Fe layers observed on 28 May 2011 at McMurdo [3], and it is comparable with the semidiurnal tide phase speed around 1 m/s calculated by the Global Scale Wave mode, GSWM09 [14], as showed in Figure 2(b). The semidiurnal tide computed by GSWM09 includes both migrating and nonmigrating components with wavenumber from -6 to $+6$. Like the tidal amplitudes in the thermospheric K layer case at Arecibo [6], the semidiurnal amplitude dominates over that of the diurnal tide in the thermosphere. Compared to the thermal tides at Arecibo, the amplitudes of the diurnal and semidiurnal tides in June at McMurdo are smaller by a scale factor of roughly 0.2, because of lack of thermal forcing [15]. It suggests less influences imposed by the thermal tides on the formation of the thermospheric Fe layers.

The second diurnal thermospheric Fe layer case is from Lübken et al. [2011]. By taking a 24-h Fe density composite 171 hours observations within a period of 12 days, Lübken et al. [2011] presented a contour plot of daily relative Fe density

perturbations from 75 to 130 km. Diurnal tidal perturbation is found in the main Fe layer from ~75 km to ~108 km, with an estimated tidal phase speed of ~5.4 m/s and a vertical wave length of ~36 km. Above 108 km, the positive phase of the Fe density perturbations dramatically changed and the shape becomes virtually vertical, indicating large descent rate of the Fe layer center. The descent rate of the positive perturbations is faster than 10 km/h, which obviously is not consistent with the classical tidal phase speed in altitudes at polar region.

Unlike those thermospheric metal layers with tidal features in mid and low latitudes [6, 7, 8], the two diurnal cases discussed here in polar region show complex layer envelope rather than just simple tidal shapes. As pointed out by Chu et al. [2016], the diurnal variations of the convection electric field probably play essential roles in the formation of the diurnal shape of thermospheric Fe layers. In the Section 3, we adopt the 1-D TIFE model to investigate the relative contribution of polar electric fields and tidal waves to the formation of thermospheric Fe layers in polar region.

3. SIMULATIONS OF DIURNAL CYCLES

3.1 Setup of Numerical Simulations

The numerical TIFE model is developed from first principles by Yu and Chu at the University of Colorado Boulder [5]. It is one-dimension model used to explore the formation and evolution of TIFE layers and related transport and convergence of Fe^+ in the E-F regions. The model includes the Fe and molecular ion chemistry in the E-F regions with newest reaction rate coefficients. A high-order flux corrected transport scheme is adopted to more accurately simulate the layer shapes.

In this paper, we try to reproducing the In this paper, we try to reproduce the TIFE layers observed on 18-20 June 2014 at McMurdo. Our major purpose is to investigate the roles of tidal winds and convection fields; therefore, we utilize the same initial Fe/Fe^+ profiles and auroral input as in Chu and Yu [2017]. The neutral winds including zonal and meridional winds are generated by the GSWM09, as shown in Figure 3. The interplanetary magnetic field (IMF) and solar winds data are taken from ACE satellites, and the electric field computed by Weimer-2005 is shown

in Figure 3(a). As argued in Chu and Yu [2017], we reduce the electric field strength to 25% of the original Weimer field for simulations shown in Figure (3b) and 5-6. The neutral and ionic parameters are input from MSIS and IRI models for the specific date and geomagnetic conditions.

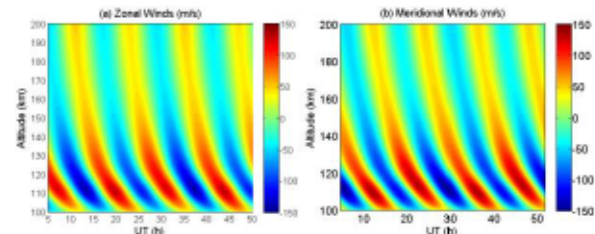


Fig. 3. Zonal (a) and meridional winds generated by the GSWM09 with monthly mean amplitude of the diurnal and semidiurnal tides in June over McMurdo.

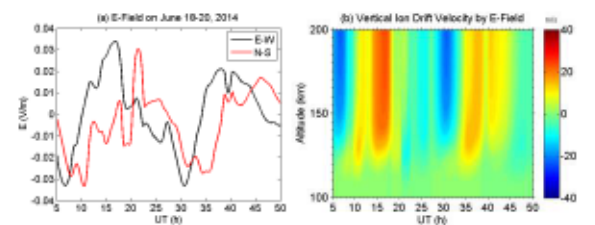


Fig. 4. The electric field (a) on June 18-20 2014 calculated from Weimer-2005 model at McMurdo, and the vertical ion drift velocity driven by electric field.

3.2 Reproducing the case on June 18-20 2014

The simulation starts at 4 UT on June 18 and runs for 48 hours. The chemistry and GLOW model are turned on for the entire period of simulations. Two scenario simulations have been tested: (1) Fe^+ and Fe transported only by the electric field, (2) Fe^+ and Fe transported by the GSWM09 winds and the electric field.

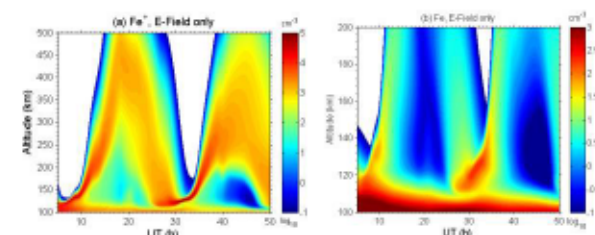


Fig. 5. The TIFE model simulations of diurnal variations of thermospheric Fe^+ (a) and Fe (b) layers transported only by the electric field.

The patterns of Fe^+ and Fe layers on June 18-20 2011 are presented in Figure 5 when the electric field is turned on but neutral winds are turned off. As shown in Figure 4(b), the ion drift velocity is downward above ~140 km, and upward below it

from 5 UT to 10 UT, leading a converged layer around ~140 km. The upward transport from 10 UT to 20 UT lift the entire layer up to F region, and then move downward by the downward transport from 20 UT to 24 UT. Similar Fe^+ layer movement is found for the next 24 hours. Eventually the Fe^+ layers exhibit periodical patterns, producing the Fe layers with upward and downward movement, as shown in Figure 5(b).

Figure 6 shows the patterns of Fe^+ and Fe layers under the same conditions as that of Figure 5 except the GSWM09 winds are turned on. Similarity between the overall envelope of Fe^+ layer in Figures 5(a) and 6(a) is found, but below 150 km, several newly converged Fe^+ layers around 12 UT, 24 UT, 36 UT and 48 UT are formed by the tidal winds, which do not occur in Figure 5(a). The Fe layers are formed from the tidal-wind-converged Fe^+ correspondingly as in Figure 6(b), although Fe layers in Figure 6(b) show similar envelope as those in Figure 5(b).

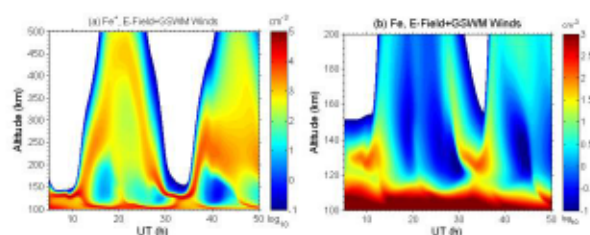


Fig. 6. The TIFe model simulations of the diurnal variations of thermospheric Fe^+ (a) and Fe (b) densities transported by the GSWM09 winds and electric fields simultaneously. The other setup parameters are the same as that of the Figure 5.

4. DISCUSSION AND OUTLOOK

The simulations presented in Figure 5 and Figure 6 suggest that the electric field is the dominant factor determining the periodic occurrence and envelopes of the thermospheric Fe^+ and Fe layers, and the diurnal and semidiurnal thermal tidal winds have minor contributions. However, the large amplitude of the semidiurnal tides below 120 km is still able to significantly shape the Fe^+ layers via relatively strong neutral-ion coupling, eventually produces tides wave-shaped Fe layers.

In this study, the winds generated by the gravity waves are not included. The simplified tidal wind inputs probably lead to the large discrepancies between the simulated and observed Fe layers. In addition, the simulated Fe^+ and Fe layers are

under the ideal assumptions of constant auroral input, zero meteor ablation input and horizontal homogeneity, which can be hardly satisfied, especially for the long simulation time. In the future, a sophisticated wind model including the gravity wave perturbations will be embedded to the TIFe model. The time varying auroral particle precipitations and meteor inputs will be taken into account for further numerical simulations.

ACKNOWLEDGEMENTS

We appreciate Jeffrey Forbes, Art Richmond and John Plane for their contributions to the TIFe model development. We thank Xiaoli Zhang for her assistance in the GSWM09 setup. This work was supported by NSF grants OPP 1246405 and 1443726.

REFERENCES

- [1] F. T. Djuth, L. D. Zhang, D. J. Livneh, I. Seker, S. M. Smith, M. P. Sulzer, J. D. Mathews, and R. L. Walterscheid, *JGR*, 115, A08305 (2010).
- [2] S. L. Vadas, *JGR*, 112, A06305 (2007).
- [3] X. Chu, et al., Lidar observations of neutral Fe layers and fast gravity waves in the thermosphere at McMurdo, Antarctica, *Geophys. Res. Lett.*, 38, L23807 (2011).
- [4] X. Chu and G. Papen, Chapter 5 in "Laser Remote Sensing", ISBN: 0-8247-4256-7, pp. 179-432 (2005).
- [5] X. Chu and Z. Yu, Formation mechanisms of neutral Fe layers in the thermosphere at Antarctica studied with a TIFe model, *J. Geophys. Res.*, 122, 6812-6848 (2017).
- [6] J. S. Friedman, X. Chu, C. Brum and X. Lu, *J. Atmos. Sol. Terr. Phys.* (2013).
- [7] Q. Gao, X. Chu, X. Xue, X. Dou, T. Chen, and J. Chen, *JGR Space Physics*, 120(10), 9213–9220 (2015).
- [8] A. Z. Liu, Y. Guo, F. Vargas, and G. R. Swenson, *GRL*, 43, 2374–2380 (2016).
- [9] Lübken, F.-J., J. Höffner, T. P. Viehl, B. Kaifler, and R. J. Morris, *Geophys. Res. Lett.*, 38, L24806, (2011).
- [10] Höffner, J., and J. S. Friedman, *Atmos. Chem. Phys.*, 4, 801–808 (2004).
- [11] Höffner, J., and J. S. Friedman, *J. Atmos. Sol. Terr. Phys.*, 67, 1226–1237 (2005).
- [12] X. Chu, Z. Yu, W. Fong, C. Chen, J. Zhao, I. F. Barry, J. A. Smith, X. Lu, W. Huang, and C. S. Gardner, invited paper in *Proceedings of the 27th International Laser Radar Conference*, New York, July 2015 (2016).
- [13] X. Chu, et al., Antarctic Fe and Na lidars: laser spectroscopy in space for exploring cosmic dust and gravity waves, *Proceedings of the 29th International Laser Radar Conference*, Hefei, July 2019 (to be published).
- [13] X. Zhang, J. M. Forbes, and M. E. Hagan, *JGR*, Vol 115, A06317 (2010).
- [15] M. E. Hagan and J. M. Forbes, *JGR*, Vol. 108, NO. A2, 1062 (2003).
- [16] T. T. Tsuda, X. Chu, T. Nakamura, M. K. Ejiri, T. D. Kawahara, A. S. Yukimatu, and K. Hosokawa, *GRL*, 42, 3647-3653 (2015).